Chinese Journal of Aeronautics, (2015),28(2): 447–456

Chinese Society of Aeronautics and Astronautics
& Beihang University

Chinese Journal of Aeronautics

cja@buaa.edu.cn
www.sciencedirect.com

Drop test and crash simulation of a civil airplane fuselage section

Liu Xiaochuan [a,*], **Guo Jun** [b], **Bai Chunyu** [b], **Sun Xiasheng** [b], **Mou Rangke** [b]

[a] *School of Aeronautics, Northwestern Polytechnical University, Xi'an 710072, China*
[b] *Aircraft Strength Research Institute, Xi'an 710075, China*

Received 21 May 2014; revised 12 August 2014; accepted 12 November 2014
Available online 7 March 2015

KEYWORDS

Civil airplane;
Drop test;
Finite element method;
Fuselage section;
Rivet failure

Abstract Crashworthiness of a civil airplane fuselage section was studied in this paper. Firstly, the failure criterion of a rivet was studied by test, showing that the ultimate tension and shear failure loads were obviously affected by the loading speed. The relations between the loading speed and the average ultimate shear, tension loads were expressed by two logarithmic functions. Then, a vertical drop test of a civil airplane fuselage section was conducted with an actual impact velocity of 6.85 m/s, meanwhile the deformation of cabin frame and the accelerations at typical locations were measured. The finite element model of a main fuselage structure was developed and validated by modal test, and the error between the calculated frequencies and the test ones of the first four modes were less than 5%. Numerical simulation of the drop test was performed by using the LS-DYNA code and the simulation results show a good agreement with that of drop test. Deforming mode of the analysis was the same as the drop test; the maximum average rigid acceleration in test was 8.81*g* while the calculated one was 9.17*g*, with an error of 4.1%; average maximum test deformation at four points on the front cabin floor was 420 mm, while the calculated one was 406 mm, with an error of 3.2%; the peak value of the calculated acceleration at a typical location was 14.72*g*, which is lower than the test result by 5.46%; the calculated rebound velocity result was greater than the test result 17.8% and energy absorption duration was longer than the test result by 5.73%.

1. Introduction

Crashworthiness is one of the key performances of civil airplane structure safety. Fuselage structure plays an important role in absorbing the kinetic energy during crash. Through the deformation, crushing and damage of sub-floor structure, a survivable space inside the cabin area should be preserved, exit should be kept clear, and the impact forces transmitted to the passengers must be reduced below the human injury tolerance.

* Corresponding author. Tel.: +86 29 88268229.
E-mail addresses: asri02@163.com (X. Liu), baichunyu2006@163.com (C. Bai), sunxs623@avic.com.cn (X. Sun).
Peer review under responsibility of Editorial Committee of CJA.

Production and hosting by Elsevier

http://dx.doi.org/10.1016/j.cja.2015.01.007

Full-scale fuselage section structure drop test is the most direct method, yet the most expensive one to evaluate the crashworthiness of the fuselage structure. Understanding and explanation of the test data provide a basis for improving crashworthiness performance of aircraft components. Since there is high nonlinearity during the crash kinetic energy absorption, which includes geometric and material nonlinearity, the crash modeling and numerical method must be validated by the test results. The validated crash analysis model can be used to evaluate crashworthiness in other impact conditions, thus reducing the needs for extensive drop tests. Furthermore, a validated modeling method is also useful as a basis for simulation of other similar airframe structures.

The Federal Aviation Administration (FAA) and National Aeronautics and Space Administration (NASA) did a series of drop tests and simulation method studies of transport airplane fuselage section.[1–6] National Aerospace Laboratory of Japan performed vertical impact test and simulation of YS-11A airliner fuselage section.[7] Ren et al.[8] studied the effect of cabin-floor oblique strut on the crashworthiness of typical civil aircraft fuselage section. Most compounds of the fuselage section are assembled together by rivets, and studies show that the dynamic failure load of the rivets, which was related to the loading speed, could affect the impact deforming mode and dynamic response.[9–11]

In this paper, an isotropic elastic plastic model was used to characterize the non-linear behavior of the rivet. Pure tension and shear failure load tests were performed with different values of speed to define the failure criterion of a rivet.

Drop test of a civil airplane fuselage section with 7 frames, about 2.93 m long, equipped with seats, overhead bins and test dummies was conducted, with a preconcerted impact velocity of 7 m/s. Deformations of the structure and accelerations at typical locations were measured and used to validate the modeling method and numerical method of impact simulation.

A finite element model of the main fuselage structure was developed and validated by the mode test results. Then a drop test analysis model was developed by assembling the validated main structure finite element model with seats, test dummies, overhead bins, high-speed camera and data acquisition system (DAS) brackets, and adjusting the initial condition. Numerical simulation of the drop test was performed by using the LS-DYNA explicit finite element code. The simulation results were compared with the drop test results, showing that the simulation results fit well with the drop test results.

2. Dynamic failure of rivet

2.1. Failure model

In the current studies, the rivets were modeled as one-dimensional element with isotropic elastic plastic model.[12,13] The non-linear behavior and the failure criterion are expressed by

$$\left[\frac{N(\alpha)}{N_u}\right]^a + \left[\frac{T(\alpha)}{T_u}\right]^b \leqslant 1 \tag{1}$$

where $N(\alpha)$ and N_u are the current and the ultimate tensile components respectively, and $T(\alpha)$ and T_u are the current and the ultimate shear components respectively. The global load, F, may be divided into two components as a function of the angular position: $N(\alpha) = F\cos\alpha$ and $T(\alpha) = F\sin\alpha$. A variation of the angular position leads to different load configurations, for example, $\alpha = 0°$ and $\alpha = 90°$ correspond to pure tensile and pure shear condition, respectively.

In this paper, a and b are set to 2. If the failure criterion calculated by current tension load and shear load is less than 1.0, the rivet joint could be treated as a rigid connection, when the current failure criterion is greater than 1.0, the rivet joint fails, then the stiffness between the two riveted nodes is set to zero.

2.2. Test setup and test results

The type of rivet for test is MS20470AD6, a full head rivet, which has a diameter of 6/32 inch (1 inch = 25.4 mm) and is made of aluminum alloy 2117-T4.

The tests are performed at $\alpha = 0°$ and $\alpha = 90°$, and the maximum impact velocity of recent conducted civil airplane fuselage drop test is 9.13 m/s,[1,4,7] so the failure criteria of the rivet are characterized with loading speed up to 10 m/s, and the loading speeds are quasi-static, 0.3, 1.0, 5.0 m/s, 10.0 m/s. Quasi-static test is performed with servo-hydraulic machine (model INSTRON 8801-4). Dynamic test is performed with INSTRON VHS8800, which is equipped with high capacity valves, enabling generating the tension and compression speed up to 20 m/s.

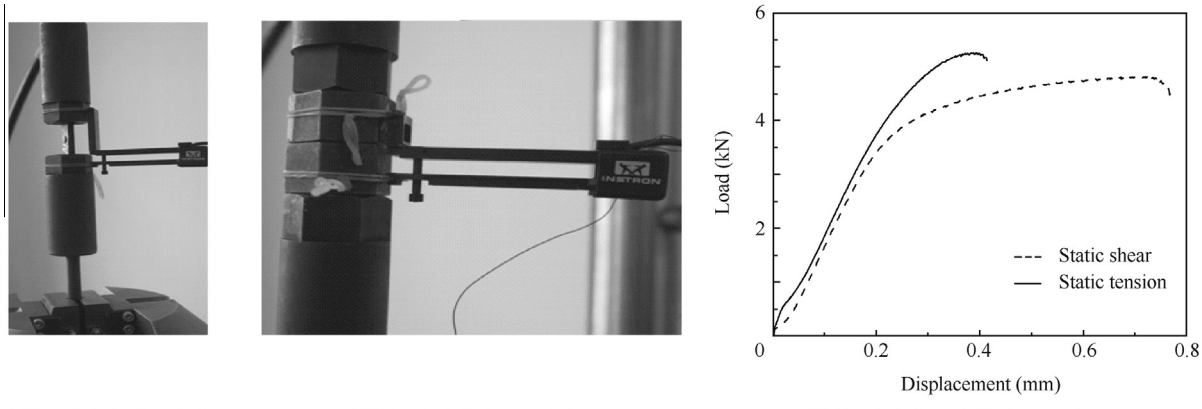

(a) Quasi-static shear test (b) Quasi-static tension test (c) Quasi-static load-displacement curve

Fig. 1 Photograph of quasi-static shear and tension tests of the rivet.

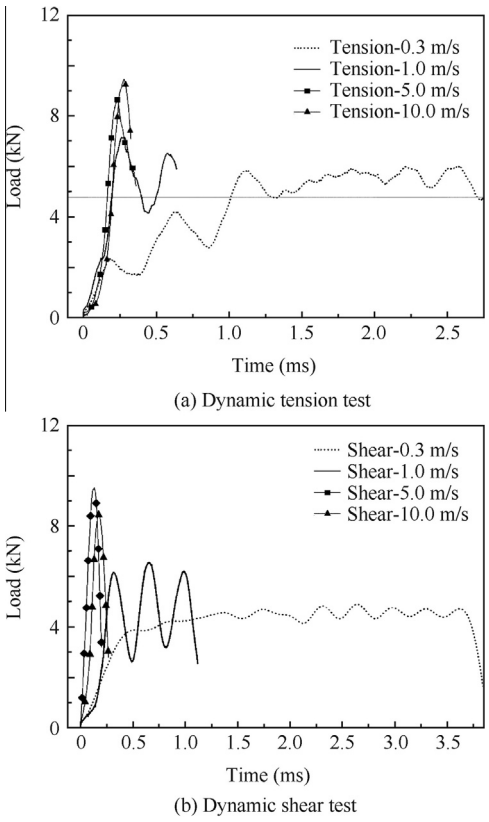

Fig. 2 Unfiltered typical dynamic tension and shear load-time curves.

The test jig is fabricated with high strength steel alloy, and the dynamic load is measured by the strain gauges located on the lower part of the jig. The two pieces of jig are assembled as a specimen by a rivet. A photograph of the quasi-static test setup and typical quasi-static force-displacement curves is shown in Fig. 1, typical dynamic tension and shear force versus time curves are shown in Fig. 2. At least three effective tests are conducted at each shear and elongation speed, and the average ultimate tension and shear loads at different speeds are shown in Table 1.

Directly enough, the relation between the test loading speed (m/s) and the average ultimate tension load (kN) can be expressed by a logarithmic function:

$$N_u = 1.095 \ln v + 7.61 \quad (2)$$

The relationship between the test loading speed and the average ultimate shear load can be expressed by

$$T_u = 1.155 \ln v + 7.27 \quad (3)$$

Table 1 Average ultimate tension and shear loads.

Speed (m/s)	Average ultimate tension load (kN)	Average ultimate shear load (kN)
Quasi-static	5.22	4.83
0.3	6.16	5.65
1.0	7.89	7.74
5.0	9.10	8.76
10.0	10.25	10.07

3. Fuselage section drop test

The vertical drop test of the fuselage section was conducted at Structure Drop Test Facility in ASRI (Airplane Strength Research Institute, Xi'an, China), 24 August, 2012.[14]

3.1. Test article

The test article is a 2.93 m long transport aircraft fuselage section with 7 frames. The outer floor beams at each end of the section are reinforced to minimize the open-end effect. The section is equipped with seats and overhead bins. Nonstructural interior liners and insulation are not equipped. Four brackets located on the upper side of the section are designed for maneuvering the test article.

The cabin section is configured with three triple cabin seats and three dual seats, placed in three rows. Fifteen 50th Hybrid III anthropomorphic test dummies (ATDs) are placed on board, each seat contained an ATD, which has a weight of 165 lb (1 lb = 0.45359 kg). Each passenger's package was simulated by replacing it with a 5 kg mass.

The ATDs are restrained in the seats by individual lower torso straps. Four of them (which are placed in the central row seats) are instrumented with load cells to measure spinal column axial loading at the lumbar and femur areas, accelerometers are placed to measure acceleration in the head and pelvic region, belt load sensors are also used to measure tension load on the safety belts.

The fuselage section is instrumented with 46 accelerometers to measure the acceleration on the cabin area, including the cabin floor and the area above it. Twenty accelerometers in the cabin floor are located close to the cross point of the seat tracks and floor beams. Another 20 accelerometers in the area above the floor are located on the sidewall fame section at three levels: seat cushion plane, overhead bin floor, and the crown area. Six accelerometers are located in overhead bin. All accelerometers are uniaxial and gravitation direction is set to positive.

Four onboard cameras and one onboard DAS are placed in the article by specially designed mounting bracket. Net weight of the test article is about 1935 kg. A photograph showing the fuselage section that is lifted to the correct drop height (prior to release) is shown in Fig. 3.

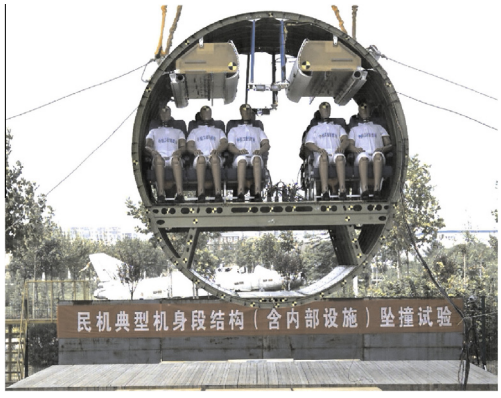

Fig. 3 Pre-test photograph of test article.

3.2. Test facility and test method

The drop test facility is made of four 20 m vertical steel towers connected on the top by a horizontal frame. An electrical winch is mounted on the frame and attached to a reeved hoisting cable, in order to maneuvering the test article. A sheave block assembly hanging from the free end of the reeved cable is attached to a solenoid-operated release hook. Below the winch cable assembly and between the tower legs, there is a 6 m by 4 m wooden platform that rests upon steel beams supported by 12 load cells.

The preconcerted impact velocity of the drop test is 7 m/s. Four cables are attached to the brackets located on the upper side of the fuselage section prior to the test, and they are adjusted to level the section in pitch and roll motions. Then the fuselage section is lifted through its center of gravity to a height of 2.5 m above the platform surface. Four soft guide ropes are used to steady the section while it was hanging above the platform.

When the test article is steady and leveled, a signal is sent to the hook to release the article, and high-speed film cameras, video cameras and the DAS are also triggered by the automatic timing sequence. Cameras and DAS are stopped when the section is steady on the platform surface after impact.

Nine high speed cameras are used to record the test at a rate of 1000 frame/s. Four of them are mounted onboard to record the internal impact reactions. The remaining five cameras are located around the exterior of the fuselage to record the dynamic deformation of the section during impact. DAS is set to record all the channels of data simultaneously with 10000 samples per second per channel. The DAS and high-speed cameras are synchronized to each other.

The impact velocity is measured and calculated by using four image makers installing on the front cabin beam, hence the average rebound velocity of the cabin floor and the deformation of sub-floor structure are obtained.

3.3. Test results

Actual impact velocity is 6.85 m/s, with a final rolling angle of 1.29°. Deformation of the test article is shown in Fig. 4, and the sub-floor structures of the section suffered a severe impact leading to a plastic deformation of some frames. And locally

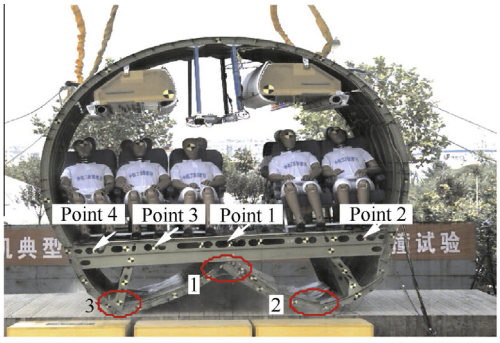

Notes: 1 — Structure crack and joint failure
2 — Plastic deform and plastic hinge
3 — Compresses.

Fig. 4 Structure deformation after impact.

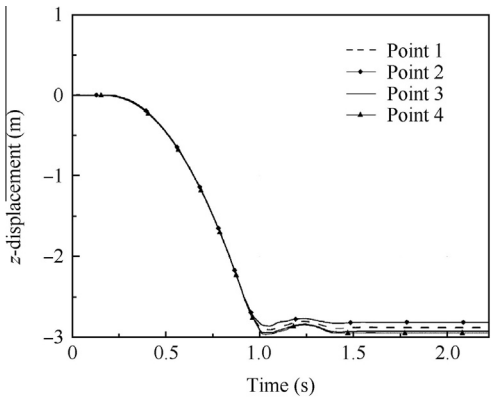

Fig. 5 Deformation of four image markers.

struts' buckle is spotted. The joints between cargo floor and frame are pulled out. The cargo beams are broken. The horizontal joints between overhead bins and frames failed, but the vertical joints remain attached, the doors of overhead bins keep closed, none of the simulated packages was dropped out. All seats remain attached at their joining points. None of the interior items affect the evacuation path for passengers. ATDs are restrained on the seats by the safety belts without heavy impact on the structure. Cabin area keeps its structural integrity.

Deformation curves of the four image markers are shown in Fig. 5.

4. Numerical simulation of fuselage section drop test

Full-scale fuselage section drop test is rather expensive and non-repeatable and the explicit non-linear dynamic finite element method is now widely used in solid materials' impact applications. After the drop test, a numerical model of the tested fuselage section is developed to reproduce the drop test results.

4.1. Modeling of fuselage section

The finite element model of the fuselage section is constructed based on the CAD model of the test article. Shell elements are used to model the fuselage skin, frames, floor and its supporting beams, high speed camera and DAS brackets, as well as the cargo floor, struts, longitudinal stringers, the fore and aft floor reinforcements. Shell element has the advantage of simulating flange bucking and crippling during impact with higher accuracy and higher accuracy in calculating the internal energy absorption, while CPU cost remains affordable. Shell elements are also used to model the two overhead bins and the frame structure of seats.

Cutouts in the fuselage skin are used to represent the windows on both sides of the section and the stiffened structure surrounding the windows is modeled using beam elements.

The metallic material formulations of the section are chosen as simplified Johnson-Cook model, MAT98 of LS-DYNA, where A, B, C and n are input material constant, and the ultimate effective failure strain is represented as materials' failure criterion. A list of material formulations' parameters of these metallic materials is provided in Table 2.

Table 2 Material of fuselage section.

Component	Density ρ (kg/m^3)	Elastic modulus E (GPa)	A (MPa)	B (MPa)	n	C	Effective failure strain ε_y (%)
Window frame	2768	71	418	696	0.837	0.004	7
Upper skin panel stringer	2770	71	309	435	0.532	0.009	15
Lower skin panel stringer	2796	71	441	608	0.792	0.006	8
Skin	2796	71	328	466	0.622	0.001	15
Frame	2796	71	475	258	0.500	0.003	8

Table 3 Material of cabin and cargo floor.

Component	Density ρ (kg/m^3)	Elastic modulus E (MPa)	Yeild stress σ_y (MPa)	Effective failure strain ε_y (%)
Cabin floor	299	18	222	0.01
Cargo floor	497	40	178	0.02

Table 4 Mode test and analytical result of the main fuselage structure.

Mode No.	Frequency (Hz)		Error (%)
	Analysis	Test	
1	10.90	10.87	0.28
2	17.86	18.69	−4.44
3	18.69	19.34	−3.16
4	22.71	21.65	4.90

The cabin floor and cargo floor are made of composite materials, formulated with ideal elastic-plastic model. A list of equivalent material properties of these composite materials is provided in Table 3.

Components of the fuselage section are assembled by rigid joints and the weight of the finite element model without seats, overhead bins, ATDs, high-speed camera and DAS brackets is 405 kg, which is 1.2% lighter than the real structure.

Free-free modes' test and mode analysis of the fuselage section without seats, overhead bins and other cabin items are performed, the fuselage section is suspended with elastic string at the four brackets, 48 accelerometers are used to measure the response of structure, and the modal parameter is identified with multiple random excitation. As shown in Table 4, the frequency errors between analysis and test of the first four modes are less than 5%, which confirm that the stiffness and mass distributions of the finite element model are valid in representing the real main fuselage structure.

4.2. Numerical simulation of fuselage section drop test

Numerical simulation of the drop test is performed by using LS-DYNA explicit FE code.[15] Studies show that initial impact velocity, impact position, inertia characters, rivet failure and contact have strong effect on the impact analysis results.[16,17]

The simulation model is prepared by assembling the fuselage section structure, seats, overhead bin, high-speed camera and DAS brackets. And the initial conditions of the finite element model, including the impact velocity and positions, are adjusted the same as the drop test conditions. The seats' legs are fixed at the same locations in the test article, and the passenger's packages are substituted by equivalent mass, 5 kg for each passenger.

To avoid negative volume and self-penetration, modeling of the seat cushion foam needs solid element with rather small mesh size and special calculation method, which would make the numerical simulation too complex to get the structural deformation and response which we concern most, so the cushion is modeled as non-structural mass. The ATD is simplified as 1D mass situated at the seat reference point, connected to the seat tube rigidly. Inertia load of the ATD during the impacting is transferred to the seats' tube and then transferred to the cabin floor beam.

A rigid surface is used to simulate the wooden plate, and the edge nodes of the rigid surface are fixed. The overall finite element model consists of 246540 nodes, 278962 shell elements, and 691 beam elements. The total weight of the model is 1913 kg, which is slightly lighter than the test article (1935 kg). The finite element model of the test article is shown in Fig. 6.

A master-surface to slave-node contact is defined between the impact surface and the nodes forming the lower part of the fuselage section. An automatic contact surface is defined between sub-floor structure to prevent the fuselage section nodes and elements from passing through the cabin floor as their deformation during the impact.

The rivet joints below the area where struts are mounted with the frame are modeled by spot-weld elements with a

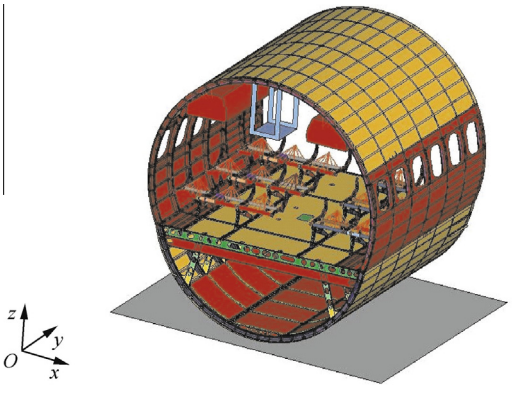

Fig. 6 Finite element model of test article.

force-based failure criterion given in Eq. (1); the ultimate tension load and ultimate shear load are calculated from Eqs. (2) and (3) with the drop test impact velocity, which is 6.85 m/s. Other rivets' joints are rigid connection without failure mode assigned.

In order to avoid the undesirable oscillation in contact, the viscous damping is involved and it is proportional to critical mode damping;[14] its default value zero, in this paper, by numerical testing, 40% of critical damping is given; bulk viscosity and hourglass viscosity are set to be default value; the friction between the subfloor of the fuselage and wooden impact plate would restrict the sliding of the deformed structure; referring to the friction coefficient between aluminum and hardwood and also by numerical testing, the static friction coefficient is set as 0.2 and the sliding friction coefficient is set as 0.1.

The total simulation duration is 350 ms, output time step of d3plot file is 0.5 ms, and the minimum time step is 6.7×10^{-7} s. Numerical simulation is performed on a LENOVO HPZ620 workstation and a single run of a simulation needs about 12 h.

4.3. Simulation results

The simulated structure impact deformation is shown in Fig. 7. The deforming mode and energy absorption mode of the analysis model are same with the drop test results, as shown in Fig. 4.

As shown in Fig. 7, the rivet failure model affects the structural deforming mode. The rigid joint increases local stiffness, while the joints do not fail (as shown in Fig. 7(b)), so the damage force of the subfloor structure increases, which means that more energy is dissipated before the strut impact ground.

At the same time, the rivet joints with static failure criterion decrease the local stiffness and there are more failed rivets (see Fig. 7(c)). The damage force of subfloor structure decreases, which means that less energy is dissipated before the strut impact ground.

Deformation images of the drop test and impact simulation of the fuselage section with different residual velocities are provided in Fig. 8, which indicates a good agreement between drop test and crash simulation.

Assuming the test article as a mass point, the average rigid impact acceleration can be calculated from impact load divided by the total mass. As shown in Fig. 9, when modeling the subfloor rivet joints with the given dynamic failure criterion, the maximum value (the first peak) of test average rigid acceleration is 8.81g while the analytical one is 9.17g, giving a 4.1% error. When modeling all rivet joints with rigid connection, the analytical one is 11.51g, giving a 30.6% error. When modeling the subfloor rivet joints with static failure criterion, the first peak value is 6.08g, with a −31.0% error, and the maximum value is 7.95g, with a −9.8% error.

The analytical vertical deformation curves of the four marked points are shown in Fig. 10, and the maximum and residual values of the test and analytical deformations of each point are provided in Table 5. The average maximum test deformation of the four points is greater than the analytical one by about 3.3%. The average test residual deformation, mostly reflecting the plastic deformation of the sub-floor structure, is only 0.4% larger than analysis, showing that the analytical sub-floor plastic deformation is basically the same as the test result. The test deformation curves of the four points are compared with the analytical curves, as shown in Fig. 9, concluding that the rebound height of the analytical model is greater than the test results, which means that the analytical model is stiffer than the test article.

The error of residual deformation at Point 2 and Point 4 are larger than the other two points, meaning the cabin floor rolling angle of the analytical model after impacting is less than the test results. The cabin floor rolling angle of the analysis model is 2.2°, while the drop test result is 4.13°.

As shown in Fig. 11 and Table 6, the rebound velocity in analysis is 1.25 m/s, larger than the test result by about 17.8%, meaning that the dissipated energy of the simulated result is less than the test result. And the energy absorption duration, defined as the period when the structure contacts the rigid surface to the impact velocity reduced to zero just before the clearly rebounding happens, is longer than the test result by about −2.27%.

Nodal acceleration of the finite element model at nodes fixed with concentrated mass has less numeric oscillation,[18] so the vertical nodal acceleration of a concentrated mass point, which simulates the ATD at central seat of the tri-seat of the central row, is used to compare with the ATD acceleration

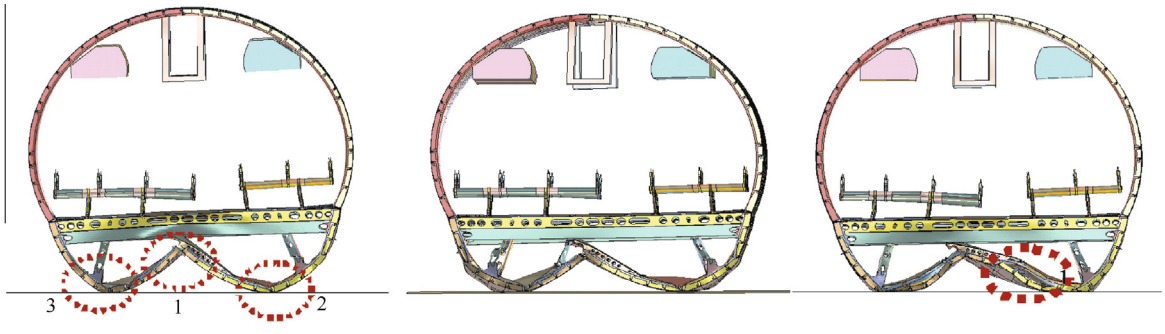

(a) Deformation with dynamic rivet failure (b) Deformation without rivet failure (c) Deformation with static rivet failure

Fig. 7 Simulated structure impact deformation.

Residual velocity (%)	Drop test	Impact simulation
80		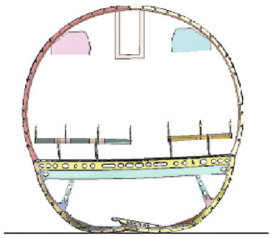
60		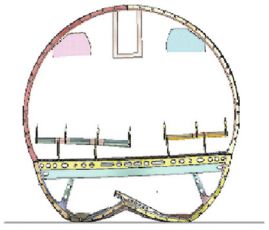
40		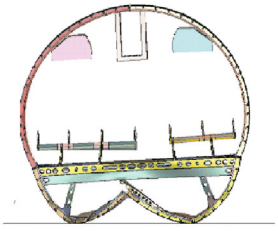
20		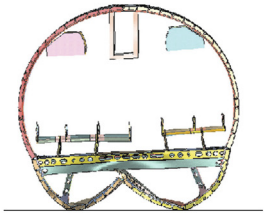
0		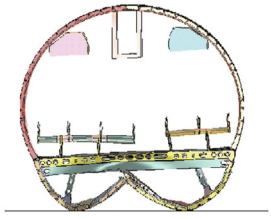

Fig. 8 Comparison of analysis and test deformations.

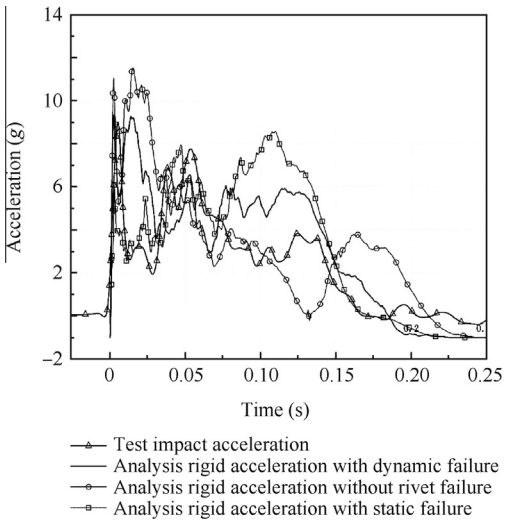

Fig. 9 Test and analytical vertical rigid accelerations.

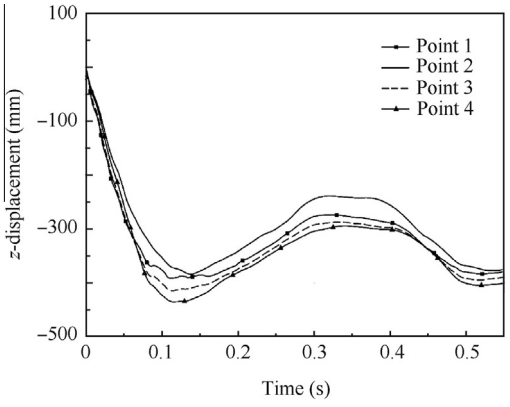

Fig. 10 Analytical displacement of four marked points.

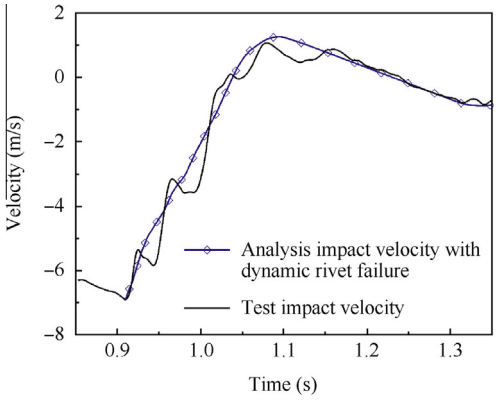

Fig. 11 Test and analytical impact velocity.

Table 6 Test and analytical Rebound velocity.

Method	Rebound velocity (m/s)	Energy absorption duration (s)
Test	1.06	0.132
Analysis	1.25	0.129
Error (%)	17.8	−2.27

at the pelvic (direction Z). Both analysis and test accelerations are filtered with CFC60.[19] The test and analytical accelerations are shown in Fig. 12; the test curve is clearly different from the analytical one, without the damping of cushion; the analytical acceleration reaches peak value just after impact, but the test result shows clear stages, and when the cushion foam is densified, the stiffness between ATD and seat is rather high; it could be assumed that the ATD is connected to the seat rigidly, so the peak value of the analytical acceleration is 14.72g, giving only a 5.46% difference to the peak value of the test acceleration.

Table 5 Test and analytical vertical deformation results of four marked points.

Location		Vertical deformation (mm)		Error (%)
		Analysis	Test	
Point 1	Maximum deformation	391.2	406.8	−3.8
	Residual deformation	383.5	380.8	0.7
Point 2	Maximum deformation	383.8	362.5	5.9
	Residual deformation	377.4	313.8	20.3
Point 3	Maximum deformation	414.6	454.4	−8.8
	Residual deformation	394.7	424.4	−7.0
Point 4	Maximum deformation	435.4	464.4	−6.2
	Residual deformation	404.6	447.7	−9.6
Average	Maximum deformation	406.3	419.8	−3.2
	Residual deformation	390.1	391.7	−0.4
C.G.	Maximum deformation	430.5		
	Residual deformation	390.0		

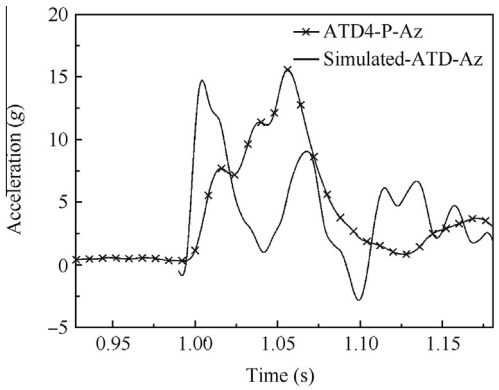

Fig. 12 Test and analytical vertical acceleration of an ATD.

5. Conclusions

(1) An isotropic elastic-plastic model is used to characterize the non-linear behavior of the rivets. Then pure tension and shear tests of a rivet are performed with different values of loading speed to define its failure criterion. Test results show that the ultimate tension and shear failure loads are strongly affected by the loading speed, and the relations between the loading speed and the ultimate failure load are expressed as two logarithmic functions.

(2) Drop test of a civil airplane fuselage section with 7 frames, about 2.93 m long, equipped with seats, overhead bins and test dummies is conducted with an impact velocity of 6.85 m/s. Deformation of the structure and acceleration at typical locations are measured. The crash kinetic energy is absorbed by plastic deformation and several structure failures are spotted. The cabin area keeps its structural integrity after impact.

(3) A finite element model of the main structure of the fuselage section is developed and validated by the mode test results. Then the drop test analytical model is prepared by assembling the validated main structure finite element model with seats, ATDs, overhead bins, high-speed camera and DAS brackets, as well as adjusting the initial condition. Numerical simulation of the drop test is performed using the LS-DYNA explicit finite element code.

(4) The fuselage section drop test simulation results are compared with the test results, showing that the analytical results fit well with the test results. Deforming mode and the deforming process of the analytical results are similar to drop test; the maximum value of test average rigid acceleration is 8.81g while the analytical one is 9.17g, with an error of 4.1%. The average maximum test deformation at four reference points on the front cabin floor is 420 mm, while the analytical one is 406 mm, with an error of 3.2%; the maximum value of the analytical acceleration of a typical location is 14.72g, lower than test result by 5.46%; Analytical rebound velocity is larger than the test result by about 17.8%, and energy absorption duration is longer than the test result by 5.73%.

(5) For a higher accurate simulation, the equivalent damping properties of cushion should be included.

Acknowledgment

This study was supported by the Ministry Level Project of China.

References

1. Abromowitz A, Smith TG, Vu T. Vertical drop test of a narrow body transport fuselage section with a conformable auxiliary fuel tank onboard. National Technical Information Service (NTIS), Springfield, Virginia 22161; 2000. Report No.: DOT/FAA/AR-00/56.
2. Abromowitz A, Smith TG, Vu T. Vertical drop test of a Shorts 3–30 airplane. National Technical Information Service (NTIS), Springfield, Virginia 22161; 1999. Report No.: DOT/FAA/AR-99/87.
3. Jackson KE, Fasanella EL. A survey of research performed at NASA Langley Research Center's impact dynamics research facility. Reston: AIAA; 1986. Report No.: AIAA-2003-1896.
4. Fasanella EL, Jackson KE. Crash simulation of a Boeing 737 fuselage section vertical drop testC. *Proceedings of the third KRASH user's conference*; 2001 Jan. Phoenix (AZ). 2001.
5. Byar A. A crashworthiness study of a Boeing 737 fuselage section [dissertation]. Philadelphia (PA): Drexel University; 2003.
6. Jackson KE, Fasanella EL. Crash simulation of vertical drop tests of two Boeing 737 fuselage sections. National Technical Information Service (NTIS), Springfeild, Virginia 22161; 2002. Report No.: DOT/FAA/AR-02/62.
7. Kumakura I, Terada H. Research plan at NAL on drop test of fuselage structure of YS-11A turbo-prop transport aircraft. *The 3rd International aircraft fire and cabin safety research conference*; 2001 Oct; Atlantic City (NJ). 2001.
8. Ren YR, Xiang JW, Luo ZP, Zheng JQ. Effect of cabin-floor oblique strut on crashworthiness of typical civil aircraft fuselage section. *Acta Aeronautica et Aatronautica Sinica* 2010;**31**(2):271–6 [Chinese].
9. San Vicente JL, Beltran F, Martinez F. Simulation of impact on composite fuselage structures. *European congress on computational methods in applied sciences and engineering*; 2000 Sep; Barcelona; 2000.
10. Deletombe E, Delsart D, Fabis J, Langrand B, Ortiz R. Recent development in modeling and test fields with respect to crashworthiness and impact on aerospace structures. *European congress on computational methods in applied sciences and engineering*; 2004 Jul; Jyvaskyla. 2004.
11. Deletombe E, Delsart D, Kohlgrüber D, Johnson AF. Improvement of numerical methods for crash analysis in future composite aircraft design. *Aerospace Sci Technol* 2000;**4**:189–99.
12. Patronelli L, Langrand B, Deletombe E, Makiewicz E, Drazetic P. Characterisation of macroscopic criterion for riveted joint failure in airframe crash simulations. *EUROPAM '99*; 1999 Oct. Darmstadt. 1999.
13. Langrand B, Patronelli L, Deletombe E. Iterative test/numerical procedure to design riveted joints for airframe crashworthiness. In: *CMEM 2001*; 2001 Jun; Alicante. Ashurst: Wessex Institute of Technology; 2001.
14. Liu X C, Guo J, Sun X S, Mou RK. Drop test and structure crashworthiness evaluation of civil airplane fuselage section with cabin interiors. *Acta Aeronaut Astronaut Sin* 2013;**34**(9):2130–40 [Chinese].
15. Jackson K E, Fasanella E L. Best practices for crash modeling and simulation. Washington, D.C.: NASA; 2002. Report No.: NASA/TM-2002-211944.
16. Ren YR, Xiang JW, Luo ZP, Zheng JQ. Crashworthiness analysis and design of aircraft fuselage structure. *Eng Mech* 2013;**30**(10):296–304 [Chinese].

17. Liu XC, Zhou SF, Ma JF, Sun XS, Mou RK. Correlation study of crash analysis and test of civil airplane sub-cabin energy absorption structure. *Acta Aeronaut Astronaut Sin* 2012;**33**(12):2202–10 [Chinese].
18. LS-DYNA (2007) Keyword user's manual, v. 971. Livermore: Livermore Software Technology Corporation; 2007.
19. Society of Automotive Engineers International. *SAE J211/1 Instrumentation for impact test—Part 1, electronic instrumentation*. New York: Society of Automotive Engineers International; 2007.

Liu Xiaochuan received his B.S degree in aircraft design engineering from Nanjing University of Aeronautics and Astronautics in 2004 and his Ph.D. degree in aircraft structure design from Northwestern Polytechnical University in 2014. His main research interests are structural impact dynamic testing and energy absorption design.

Guo Jun is a senior engineer at Aircraft Strength Research Institute of China. His main research interests are impact testing and numerical calculation.

Bai Chunyu is an engineer at Aircraft Strength Research Institute of China. His main research interests are material testing and structural fatigue.

Sun Xiasheng is a professor and Ph.D. supervisor at School of Aeronautics, Northwestern Polytechnic University. His main research interests are optimization method and light structure design.

Mou Rangke is a senior engineer at Aircraft Strength Research Institute of China. His main research interests are landing gear dynamic and energy absorption.